



1 Ubiquitous production of branched glycerol dialkyl glycerol tetraethers (brGDGTs) in
2 global marine environments: a new source indicator for brGDGTs

3 Wenjie Xiao^{1,2}, Yinghui Wang², Shangzhe Zhou², Limin Hu³, Huan Yang⁴, Yunping Xu^{1,2*}

4 ¹Shanghai Engineering Research Center of Hadal Science and Technology, College of Marine
5 Sciences, Shanghai Ocean University, Shanghai 201306, China

6 ²MOE Key Laboratory for Earth Surface Process, College of Urban and Environmental Sciences,
7 Peking University, Beijing 100871, China

8 ³Key Laboratory of Marine Sedimentology and Environmental Geology, First Institute of
9 Oceanography, State Oceanic Administration, Qingdao 266061, China

10 ⁴State Key Laboratory of Biogeology and Environmental Geology, China University of Geosciences,
11 Wuhan 430074, China

12 Corresponding author: Y Xu (ypxu@shou.edu.cn)

13

14 Abstract. Presumed source specificity of branched and isoprenoid glycerol dialkyl
15 glycerol tetraethers (GDGTs) led to the development of several biomarker proxies for
16 biogeochemical cycle and paleoenvironment. However, recent studies reveal that
17 brGDGTs are also produced in aquatic environments besides soils and peat. Here we
18 examined three cores from the Bohai Sea and found distinct difference in brGDGT
19 compositions varying with the distance from the Yellow River mouth. We thus proposed
20 an abundance ratio of hexamethylated to pentamethylated brGDGT (IIIa/IIa) to
21 evaluate brGDGT sources. The compiling of globally distributed 1354 marine
22 sediments and 589 soils shows that the IIIa/IIa ratio is generally <0.59 for soils, 0.59–
23 0.92 and >0.92 for marine sediments with and without significant terrestrial inputs,
24 respectively. Such disparity confirms the existence of two sources of brGDGTs, a
25 terrestrial origin with lower IIIa/IIa and a marine origin with higher IIIa/IIa, likely due
26 to different pH influence. The application of the IIIa/IIa ratio to the East Siberian Arctic
27 Shelf proves it a sensitive source indicator for brGDGTs, which is helpful for accurate



28 estimation of organic carbon source and paleoclimates in marine settings.

29

30 1 Introduction

31 Glycerol dialkyl glycerol tetraethers (GDGTs), membrane lipids of archaea and
32 certain bacteria, are widely distributed in marine and terrestrial environments
33 (Reviewed by Schouten et al., 2013). These lipids have become a focus of attention of
34 organic geochemists for more than ten years because they can provide useful
35 environmental and climatic information such as temperature, soil pH, organic carbon
36 source and microbial community structure (e.g., Hopmans et al., 2004; Kim et al., 2010;
37 Lipp et al., 2008; Peterse et al., 2012; Schouten et al., 2002; Weijers et al., 2006; Zhu
38 et al., 2016). There are generally two types of GDGTs, isoprenoid (iGDGTs) and non-
39 isoprenoid, branched GDGTs (brGDGTs; Fig. 1). The former group is more abundant
40 in aquatic settings and generally thought to be produced by Thaumarchaeota, a specific
41 genetic cluster of the archaea domain (Schouten et al., 2008; Sinninghe Damsté et al.,
42 2002), although Euryarchaeota may be a significant source of iGDGTs in the ocean
43 (e.g., Lincoln et al., 2014). In contrast, brGDGTs having 1,2-di-*O*-alkyl-*sn*-glycerol
44 configuration are substantially more abundant in peat and soils than marine sediments,
45 supporting that they are derived from bacteria rather than archaea (Sinninghe Damsté
46 et al., 2000; Weijers et al., 2006). So far, only two species of Acidobacteria were
47 identified to contain one brGDGT with two 13,16-dimethyl octacosanyl moieties
48 (Sinninghe Damsté et al., 2011), which is contrast to high diversity and ubiquitous
49 occurrence of a series of brGDGTs with four to six methyl groups and zero to two
50 cyclopentane rings in environments (Weijers et al., 2007b). Therefore, other biological
51 sources of brGDGTs, although not yet identified, are likely.

52 The source difference between brGDGTs and iGDGTs led researchers to
53 developing a branched and isoprenoid tetraether (BIT) index, expressed as relative
54 abundance of terrestrial-derived brGDGTs to aquatic-derived crenarchaea (Hopmans et
55 al., 2004). Subsequent studies found that the BIT index is specific for soil organic
56 carbon because GDGTs are absent in vegetation (e.g., Sparkes et al., 2015; Walsh et al.,



57 2008). The BIT index is generally higher than 0.9 in soils, but close to 0 in marine
58 sediments devoid of terrestrial inputs (Weijers et al., 2006). Since its advent, the BIT
59 index has been increasingly used in different environments (e.g., Blaga et al., 2011;
60 Herfort et al., 2006; Kim et al., 2006; Loomis et al., 2011; Wu et al., 2013). Besides the
61 BIT index, Weijers et al. (2007b) found that the number of cyclopentane moieties of
62 brGDGTs, expressed as Cyclization of Branched Tetraethers (CBT), correlated
63 negatively with soil pH, while the number of methyl branches of brGDGTs, expressed
64 as Methylation of Branched Tetraethers (MBT), was dependent on annual mean air
65 temperature (MAT) and to a lesser extent on soil pH. The MBT/CBT proxies were
66 further corroborated by subsequent studies (e.g., Peterse et al., 2012; Sinninghe Damsté
67 et al., 2008; Yang et al., 2014a). Assuming that brGDGTs preserved in marine
68 sediments close to the Congo River outflow were derived from soils in the river
69 catchment, Weijers et al. (2007a) reconstructed large-scale continental temperature
70 changes in tropical Africa that span the past 25,000 years by using the MBT/CBT proxy.
71 More recently, De Jonge et al. (2013) used a tandem high performance liquid
72 chromatography-mass spectrometry (2D HPLC-MS) and identified a series of novel 6-
73 methyl brGDGTs which were previously coeluted with 5-methyl brGDGTs. This
74 finding resulted in the redefinition and recalibration of brGDGTs' indexes (e.g., De
75 Jonge et al., 2014; Xiao et al., 2015).

76 The premise of all brGDGT-based parameters is their source specificity, i.e.,
77 brGDGTs is only biosynthesized by bacteria thriving in soils and peat. Several studies,
78 however, observed different brGDGT compositions between marine sediments and
79 soils on adjacent lands, supporting in situ production of brGDGTs in marine
80 environments (e.g., Liu et al., 2014; Peterse et al., 2009a; Weijers et al., 2014; Zell et
81 al., 2014; Zhu et al., 2011), analogous to lacustrine settings (e.g., Sinninghe Damsté et
82 al., 2009; Tierney and Russell, 2009; Tierney et al., 2012) and rivers (e.g., De Jonge et
83 al., 2015; French et al., 2015a; Zell et al., 2015; Zhu et al., 2011). At the global scale,
84 Fietz et al. (2012) reported a significant correlation between concentrations of
85 brGDGTs and crenarchaeol ($p < 0.01$; $R^2 = 0.57-0.99$), suggesting that a common or
86 mixed source for brGDGTs and iGDGTs are actually commonplace in lacustrine and



87 marine settings. More recently, Sinninghe Damsté (2016) examined tetraethers in
88 surface sediments from 43 stations in the Berau River delta (Kalimantan, Indonesia),
89 and their result, combined with data from other shelf systems, supported a widespread
90 biosynthesis of brGDGTs in shelf sediments especially at water depth of 50–300 m.

91 In continental shelf, river is the most important conduit for transporting brGDGTs
92 from land to sea because these compounds were either below the detection level
93 (Hopmans et al., 2004) or were present at low abundance (Fietz et al., 2013; Weijers et
94 al., 2014) in atmospheric dust. In the remote ocean where no direct impact from land
95 erosion via rivers takes place, eolian transport and in situ production became the most
96 important contributors to brGDGTs. Weijers et al. (2014) found that distributions of
97 African dust-derived brGDGTs were similar to those of soils but different from those
98 of distal marine sediments, providing a possibility to distinguish terrestrial vs. marine
99 brGDGTs based on their molecular compositions. Considering these facts, we attempt
100 to develop a robust index to assess the source of brGDGTs in marine environments. In
101 order to reach this objective, we first examined three cores in the Bohai Sea which are
102 subject to the Yellow River influence to different degree and compared the source
103 discerning capability of different brGDGT parameters. We then applied the most
104 sensitive parameter to globally distributed marine sediments and soils to test its validity.
105 Our study supplies an important step for improving accuracy of brGDGT-derived
106 proxies and better understanding marine carbon cycle and paleoenvironments.

107

108 2 Material and methods

109 2.1 Study area and sampling

110 The Bohai Sea is a semi-enclosed shallow sea in northern China, extending about
111 550 km from north to south and about 350 km from east to west. Its area is 77,000 km²
112 and mean depth is 18 m (Hu et al., 2009). The Bohai Strait in the eastern portion is the
113 only passage connecting the Bohai Sea to the outer Yellow Sea. Several rivers,
114 including Yellow River, the second largest sediment-load river in the world, drain into
115 the Bohai Sea with a total annual runoff of 890×10^8 m³. One gravity core with 64 cm



116 long (M1; 37.52°N, 119.32°E) was collected in July 2011, while other two cores were
117 collected in July 2013, namely M3 (38.66°N, 119.54°E; 53 cm long) and M7 (39.53°N,
118 120.46°E; 60 cm long), respectively (Fig. 2). The sites M1, M3 and M7 are located in
119 the south, the center and the north of the Bohai Sea, respectively. The cores were
120 transported to the lab where they were sectioned at 1 or 2 cm interval. The age model
121 was established on basis of ^{210}Pb and ^{137}Cs activity, showing that these cores cover the
122 sedimentation period of less than 100 years (Wu et al., 2013 and unpublished data).

123

124 2.2 Lipid extraction and analyses

125 The samples were freeze dried and homogenized with a mortar and pestle. After
126 the addition of C_{46} GDGT (internal standard), the sediments (2–10 g) were
127 ultrasonically extracted with 25 ml dichloromethane(DCM)/methanol (3:1 v:v) for 15
128 min (3×). The combined extracts were concentrated by a rotary evaporator and
129 completely dried under a mild N_2 stream. The extracts were base hydrolyzed in 1 M
130 KOH/Methanol solution at 80 °C for 2 h. Neutral fractions were recovered by liquid-
131 liquid extraction with hexane, which were separated into two sub-fractions by 5 ml
132 hexane/DCM (9:1 v/v) and 5 ml DCM/Methanol(1:1 v/v), respectively, over silica gel
133 columns. The latter fraction containing GDGTs was filtered through 0.45 μm PTFE
134 filter before instrumental analyses.

135 The GDGTs were analyzed using an Agilent 1200 HPLC-atmospheric pressure
136 chemical ionization-triple quadruple mass spectrometry (HPLC-APCI-MS) system.
137 The polar fraction was dissolved in 300 μl hexane/EtOAc (84:16, v/v). Samples (10–
138 20 μl) were injected and the separation of 5- and 6-methyl brGDGTs was achieved with
139 two silica columns in sequence (150 mm×2.1 mm; 1.9 μm , Thermo Finnigan; USA) at
140 a constant flow of 0.2 ml/min. The solvent gradient was: 84% A (hexane) and 16% B
141 (EtOAc) for 5 min, increasing the amount of B from 16% at 5 min to 18% at 65 min,
142 and then to 100% B in 21 min. The column was flushed with 100% B for 4 min, and
143 then back to 84/16 A/B for 30 min in order to equilibrate the system. The APCI and MS
144 conditions were: vaporizer pressure of 4.2×10^5 Pa, vaporizer temperature of 400 °C,
145 drying gas flow of 6 L min^{-1} , temperature of 200 °C, capillary voltage of 3500 V, and



146 corona current of 5 μ A (3.2 kV). Samples were quantified based on comparisons of the
 147 respective protonated-ion peak areas of each GDGT to the internal standard in selected
 148 ion monitoring (SIM) mode. The protonated ions were m/z 1050, 1048, 1046, 1036,
 149 1034, 1032, 1022, 1020, 1018 for brGDGTs, 1302, 1300, 1298, 1296, 1292 for iGDGTs
 150 and 744 for C_{46} GDGT.

151

152 2.3 Parameter calculation and statistics

153 The BIT, MBT, Methyl Index (MI), Degree of Cyclization (DC) of brGDGTs and
 154 weighted average number of cyclopentane moieties for tetramethylated brGDGTs
 155 ($\#Rings_{tetra}$) were calculated according to the definitions of Hopmans et al. (2004),
 156 Weijers et al. (2007b), Zhang et al. (2011), Sinninghe Damsté et al. (2009) and
 157 Sinninghe Damsté (2016), respectively.

$$158 \text{ BIT} = \frac{Ia + IIa + IIIa}{Ia + IIa + IIIa + IV} \quad (1)$$

$$159 \text{ MBT} = \frac{Ia + Ib + Ic}{Ia + IIa + IIIa + Ib + IIb + IIIb + Ic + IIc + IIIc} \quad (2)$$

$$160 \text{ MI} = 4 \times (Ia + Ib + Ic) + 5 \times (IIa + IIb + IIc) + 6 \times (IIIa + IIIb + IIIc) \quad (3)$$

$$161 \text{ DC} = \frac{Ib + IIb}{Ia + IIa + Ib + IIb} \quad (4)$$

$$162 \#Rings_{tetra} = \frac{Ib + 2 * Ic}{Ia + Ib + Ic} \quad (5)$$

163 where roman numbers denote relative abundance of compounds depicted in Fig. 1. In
 164 this study, we used two silica LC columns in tandem and successfully separated 5- and
 165 6-methyl brGDGTs. However, many previous studies (e.g., Weijers et al., 2006) used
 166 one LC column and did not separate 5- and 6-methyl brGDGTs. Considering this, we
 167 combined 5-methyl and 6-methyl brGDGT as one compound in this study, for example,
 168 IIIa denotes the total abundance of brGDGT IIIa and IIIa' in figure 1.

169 An analysis of variance (ANOVA) was conducted for different types of samples
 170 to determine if they differ significantly from each other. The SPSS 16.0 software
 171 package (IBM, USA) was used for the statistical analysis. Squared Pearson correlation
 172 coefficients (R^2) reported have an associated p value < 0.05 .

173



174 2.4 Data compilation of global soils and marine sediments

175 The dataset in this study are composed of GDGTs from 1354 globally distributed
176 soils and 589 marine sediments (Fig. 2). These samples span a wide area from 75.00°S
177 to 79.28°N and 168.08°W to 174.40°E and have water depth of 1.0 to 5521 m. The
178 marine samples are from the South China Sea (Dong et al., 2015; Hu et al., 2012; Jia et
179 al., 2012; O'Brien et al., 2014), Caribbean Sea (O'Brien et al., 2014), western equatorial
180 Pacific Ocean (O'Brien et al., 2014), southeast Pacific Ocean (Kaiser et al., 2015), the
181 Chukchi and Alaskan Beaufort Seas (Belicka and Harvey, 2009), eastern Indian Ocean
182 (Chen et al., 2014), East Siberian Arctic Shelf (Sparkes et al., 2015), Kara Sea (De
183 Jonge et al., 2016; De Jonge et al., 2015), Svalbard fjord (Peterse et al., 2009a), Red
184 Sea (Trommer et al., 2009), the southern Adriatic Sea (Leider et al., 2010), Columbia
185 estuary (French et al., 2015b), globally distributed distal marine sediments (Weijers et
186 al., 2014) and the Bohai Sea (this study). Soil samples are from the Svalbard (Peterse
187 et al., 2009b), Columbia (French et al., 2015b), China (Ding et al., 2015; Hu et al., 2016;
188 Xiao et al., 2015; Yang et al., 2013; Yang et al., 2014a; Yang et al., 2014b), globally
189 distributed soils (De Jonge et al., 2014; Peterse et al., 2012; Weijers et al., 2006),
190 California geothermal (Peterse et al., 2009b), France and Brazil (Huguet et al., 2010),
191 western Uganda (Loomis et al., 2011), the USA (Tierney et al., 2012), Tanzania
192 (Coffinet et al., 2014), Indonesian, Vietnamese, Philippine, China and Italia (Mueller-
193 Niggemann et al., 2016).

194

195 3 Results and discussion

196 3.1 Distribution and source of brGDGTs in Bohai Sea

197 Both iGDGTs including crenarchaea and brGDGTs were detected in Bohai Sea
198 sediments. For brGDGTs, a total of 15 compounds were identified including three
199 tetramethylated brGDGTs (Ia, Ib and Ic), six pentamethylated brGDGTs (IIa, IIb, IIc,
200 IIa', IIb' and IIc') and six hexamethylated brGDGTs (IIIa, IIIb, IIIc, IIIa', IIIb' and
201 IIIc'). In order to evaluate provenances of brGDGTs, we calculated various parameters
202 including the BIT index, percentages of tetra-, penta- and hexa-methylated brGDGTs,
203 #rings for tetramethylated brGDGTs, DC, MI, MBT, brGDGTs IIIa/IIa and Ia/IIa (Table



204 1). The values of the BIT index ranged from 0.27 to 0.76 in the core M1, which are
205 much higher than that in the core M3 (0.04–0.25) and the core M7 (0.04–0.18). Such
206 difference is expectable since the site M1 is closest to the Yellow River outflow, and
207 receives more terrestrial organic carbon than other two sites (Fig. 2). However, the BIT
208 index itself has no ability to distinguish terrestrial vs. aquatic brGDGTs because
209 brGDGTs and crenarchaea used in this index are thought to be specific for soil organic
210 carbon and marine organic carbon, respectively (Hopmans et al., 2004). For individual
211 brGDGTs, the core M1 is characterized by significantly higher percentage of brGDGT
212 IIa ($28\pm 1\%$) than the core M2 ($18\pm 1\%$) and the core M3 ($18\pm 0\%$; Fig. 3). We performed
213 ANOVA for a variety of brGDGTs' parameters, and the results (Table 1) show that all
214 parameters except MI can distinguish Chinese soils from Bohai Sea sediments, but only
215 the IIIa/IIa ratio can completely separate Chinese soils (0.39 ± 0.25 ; Mean \pm SD; same
216 hereafter), M1 sediments (0.63 ± 0.06), M3 sediments (1.16 ± 0.12) and M7 sediments
217 (0.93 ± 0.07) into four groups.

218 Three factors may account for the occurrence of higher IIIa/IIa ratio in the Bohai
219 Sea sediments than Chinese soils: selective degradation during land to sea transport,
220 admixture of river produced brGDGTs and in situ production of brGDGTs in sea.
221 Huguet et al. (2008; 2009) reported that iGDGTs (i.e., crenarchaea) was degraded at a
222 rate of 2-fold higher than soil derived brGDGTs under long term oxygen exposure in
223 the Madeira Abyssal Plain, leading to increase of the BIT index. Such selective
224 degradation, however, cannot explain significant different IIIa/IIa ratio between the
225 Chinese soils and Bohai Sea sediments because unlike crenarchaea, both IIIa and IIa
226 belong to brGDGTs with similar chemical structures and thus have similar degradation
227 rates. In situ production of brGDGTs in rivers is a widespread phenomenon, and can
228 change brGDGT compositions in sea when they were transported there (e.g., De Jonge
229 et al., 2015; Zell et al., 2015; Zhu et al., 2011). However, this effect is minor in the
230 Yellow River because extremely high turbidity (up to 220 kg/m³ during the flood
231 season; Ren and Shi, 1986) greatly constrain the growth of aquatic organisms. The
232 studies along lower Yellow River-estuary-coast transect suggested that brGDGTs in
233 surface sediments were primarily a land origin (Wu et al., 2014). Therefore, the



234 enhanced IIIa/IIa values in the Bohai Sea sediments is caused by in situ production of
235 brGDGTs. An increasing trend from the site M1 (0.63 ± 0.06) to M7 (0.93 ± 0.07) then to
236 M3 (1.16 ± 0.12) reflects variability in relative contribution of autochthonous (lower
237 IIIa/IIa) and allochthonous (higher IIIa/IIa) brGDGTs. The site M1 is adjacent to the
238 Yellow River mouth and receives the largest amount of terrestrial organic matter,
239 causing lower IIIa/IIa values. In contrast, the site M3 located in central Bohai Sea
240 comprises of the least amount of terrestrial organic matter, resulting in higher IIIa/IIa
241 values. The intermediate IIIa/IIa values at the site M7 is attributed to moderate land
242 erosion nearby northern Bohai Sea (Fig. 2). Such distribution pattern strongly suggests
243 that the IIIa/IIa ratio is a sensitive indicator for assessing source of brGDGTs in the
244 Bohai Sea.

245

246 3.2 Regional and global validation of brGDGT IIIa/IIa

247 To test whether the IIIa/IIa ratio is valid in other environments, we apply it to the
248 Svalbard (Peterse et al., 2009a), the Yenisei River outflow (De Jonge et al., 2015) and
249 the East Siberian Arctic Shelf (Sparkes et al., 2015). By comparing the compositions of
250 brGDGTs in Svalbard soils and nearby fjord sediments, Peterse et al. (2009a) indicated
251 that sedimentary organic matter in fjords was predominantly a marine origin. A plot of
252 BIT vs. IIIa/IIa (Fig. 4a) clearly grouped the samples into two groups which correspond
253 to soils (>0.75 for BIT and <1.0 for IIIa/IIa) and marine sediments (<0.3 for BIT
254 and >1.0 for IIIa/IIa). Another line of evidence is from De Jonge et al. (2015) who
255 examined brGDGTs in core lipids (CLs) and intact polar lipids (IPLs) in the Yenisei
256 River outflow. As the IPLs are rapidly degraded in the environment, they can be used
257 to trace living or recently living material, while the CLs are generated via degradation
258 of the IPLs after cell death (Lipp et al., 2008; White et al., 1979). The compiling of
259 brGDGTs from De Jonge et al. (2015) shows significant difference of the IIIa/IIa ratio
260 between the IPL fractions (>1.0) and CL fractions (<0.8 ; Fig. 4b). Such disparity
261 supports that brGDGTs produced in marine environments have higher IIIa/IIa values
262 because labile intact polar brGDGTs are mainly produced in situ, whereas recalcitrant
263 core brGDGTs are composed of more allochthonous terrestrial components. Sparkes et



264 al. (2015) examined brGDGTs in surface sediments across the East Siberian Arctic
265 Shelf (ESAS) including the Dmitry-Laptev Strait, Buor-Khaya Bay, ESAS nearshore
266 and ESAS offshore. The plot of BIT vs. IIIa/IIa again results into two groups, one group
267 with lower BIT values (<0.3) and higher IIIa/IIa values (0.8–2.3) mainly from ESAS
268 offshore, and another group with higher BIT values (0.3–1.0) and lower IIIa/IIa values
269 (0.4–0.9) from the Dmitry-Laptev Strait, Buor-Khaya Bay and ESAS nearshore (Fig.
270 4c). A strong linear correlation was observed between the IIIa/IIa ratio and the distance
271 from river mouth ($R^2=0.58$; $p<0.05$; Fig. 4d), in accord with the data of the BIT index
272 and $\delta^{13}\text{C}_{\text{org}}$ (Sparkes et al., 2015). All lines of evidence support that marine-derived
273 brGDGTs have higher IIIa/IIa values than terrestrial derived brGDGTs.

274 We further compile all available data in literatures representing globally
275 distributed soils and marine sediments (Fig. 5). The statistical analysis clearly showed
276 that at the global scale, the IIIa/IIa ratio was significantly higher in marine sediments
277 than soils ($p<0.05$). An exception was observed for Red Sea sediments which have
278 unusually low IIIa/IIa values (0.39 ± 0.21). The Red Sea has a restricted connection to
279 the Indian Ocean via the Bab el Mandeb. This, combined with high insolation, litter
280 precipitation and strong winds result in surface water salinity up to 41 in the south and
281 36 in the north of the Red Sea (Sofianos et al., 2002). Under such extreme environment,
282 distinct populations of Crenarchaeota may be developed and produced GDGTs different
283 from that in other marine settings (Trommer et al., 2009).

284 Overall, the global distribution of IIIa/IIa presents the highest level in many deep
285 sea sediments (2.6–5.1), the lowest level in soils (<1.0), and an intermediate level in
286 sediments from bays, coastal areas or marginal seas (0.87–2.62; Fig. 5). These results
287 are consistent with our data from the Bohai Sea, and confirm that the IIIa/IIa ratio is a
288 useful proxy for tracing the source of brGDGTs in marine sediments at regional and
289 global scales.

290 Why do soils have lower IIIa/IIa values than marine sediments? It is well known
291 that relative number of methyl groups (e.g., MBT) has a negative correlation with soil
292 pH and a positive correlation with MAT (Peterse et al., 2012; Weijers et al., 2007b).
293 The IIIa/IIa ratio is actually an abundance ratio of hexamethylated to pentamethylated



294 brGDGT, and thus may be also controlled by ambient temperature and pH of source
295 organisms. Unlike iGDGTs which is well known to be mainly produced by
296 Thaumarchaeota (Schouten et al., 2008; Sinninghe Damsté et al., 2002), the marine
297 source of brGDGTs remains elusive. Here, we assume that marine organisms producing
298 brGDGTs response to ambient temperature in a same way as soil bacteria producing
299 brGDGTs, i.e., a negative correlation between relative number of methyl group of
300 brGDGTs and ambient temperature. However, even if this hypothesis is tenable,
301 temperature is still unable to explain observed distribution patterns of the IIIa/IIa ratio
302 because both soils and marine sediments are globally distributed and their temperatures
303 (MAT vs. sea surface temperature) have no systematic difference. Alternatively, the
304 analysis of global soil data of Peterse et al. (2012) shows that the IIIa/IIa ratio has a
305 positive correlation with soil pH ($R^2=0.43$). In this study, the majority of soils are acidic
306 or neutral ($\text{pH}<7.3$) and only 8% of soils have pH of >8.0 except for those from semi-
307 arid and arid regions (e.g., Yang et al., 2014a), whereas seawater is constantly alkaline
308 with pH of 8.2 on average. With this systematic difference, bacteria living in soils tend
309 to produce higher proportions of brGDGT IIIa, whereas unknown marine organisms
310 tend to biosynthesize higher proportions of brGDGT IIa if they response to ambient pH
311 in a similar way as soil bacteria in term of biosynthesis of brGDGTs (Peterse et al.,
312 2012).

313

314 3.3 Implication of IIIa/IIa on other brGDGT proxies

315 Because brGDGTs can be produced in marine settings, they are no longer specific
316 for soil organic matter, which inevitably affects brGDGT proxies (e.g., BIT, MBT/CBT).
317 The plot of BIT vs. IIIa/IIa on basis of global dataset shows that the IIIa/IIa ratio has
318 the value of <0.59 for 90% of soil samples and >0.92 for 90% of marine sediments (Fig.
319 6). Considering this fact, we propose that the IIIa/IIa ratio of <0.59 and >0.92 represents
320 terrestrial (or soil) and marine endmembers, respectively. The BIT index has the value
321 of >0.67 for 90% of soils and <0.16 for 90% of marine sediments (Fig. 6). Overall, the
322 BIT index decreased with increasing IIIa/II values ($\text{BIT} = 1.08 \times 0.28^{\frac{\text{IIIa}}{\text{IIa}}} - 0.03$; $R^2 =$



0.77; Fig. 6), suggesting that both the IIIa/IIa and BIT are useful indexes for assessing soil organic carbon in marine settings. However, when the BIT index has an intermediate value (i.e., 0.16 to 0.67), it is not valid to determine the provenance of brGDGTs. For example, several marine samples having BIT values of ~0.35 show a large range of IIIa/IIa (0.4 to 2.4; Fig. 6), suggesting that the source of brGDGTs can vary case by case. Under this situation, the measurement of the IIIa/IIa ratio is strongly recommended.

The different IIIa/IIa values between land and marine endmembers may supply an approach to quantify the contribution of soil organic carbon in marine sediments. Similar to the BIT index, we used a binary mixing model to calculate percentage of soil organic carbon (%OC_{soil}) as follow:

$$\%OC_{soil} = \left[\frac{[IIIa/IIa]_{sample} - [IIIa/IIa]_{marine}}{[IIIa/IIa]_{soil} - [IIIa/IIa]_{marine}} \right] * 100 \quad (6)$$

Where [IIIa/IIa]_{sample}, [IIIa/IIa]_{soil} and [IIIa/IIa]_{marine} are the abundance ratio of brGDGT IIIa/IIa for samples, soils and marine sediments devoid of terrestrial influences, respectively.

We applied this binary mixing model to the East Siberian Arctic Shelf because the data of BIT, δ¹³C_{org} and distance from river mouth are all available (Sparkes et al., 2015). With the distance from river mouth increasing from 25 to >700 km, the BIT, IIIa/IIa and δ¹³C_{org} change from 0.95 to 0, 0.53 to 2.21 and -27.4‰ to -21.2‰, respectively, reflecting spatial variability of sedimentary organic carbon sources. For the BIT index, we used 0.97 and 0.01 as terrestrial and marine endmember values based on previous studies for Arctic surrounding regions (De Jonge et al., 2014; Peterse et al., 2014), which are similar to global average values (Hopmans et al., 2004). For δ¹³C_{org}, we chose -27‰ and -20‰ as C3 terrestrial and marine organic carbon endmembers (Meyers, 1997 and references therein). For the IIIa/IIa ratio, we used a global average value of marine sediments (1.6) and soils (0.24), respectively, based on this study. By applying these endmember values into Eq. 6, we calculated percentage of soil organic carbon (%OC_{soil}). We removed a few data points if their calculated %OC_{soil} were greater than 100% or below 0%. It should be noted that the endmember value will affect quantitative



352 results, but does not change a general trend of %OC_{soil}. The results based on all three
353 parameters show a decreasing trend seawards (Fig. 7). However, the %OC_{soil} based on
354 $\delta^{13}\text{C}_{\text{org}}$ is the highest ($75\pm 18\%$), followed by that from the IIIa/IIa ratio ($58\pm 15\%$) and
355 then that from the BIT index ($43\pm 27\%$). This difference have been explained by that
356 $\delta^{13}\text{C}_{\text{org}}$ is a bulk proxy for marine vs. terrestrial influence of sedimentary organic carbon
357 (SOC), whereas the BIT index is for a portion of the bulk SOC, i.e., soil OC (Walsh et
358 al., 2008) or fluvial OC (Sparkes et al., 2015). For the estimated %OC_{soil}, $\delta^{13}\text{C}_{\text{org}}$
359 presents a stronger positive correlation with the IIIa/IIa ratio ($R^2=0.49$) than the BIT
360 index ($R^2=0.45$), suggesting that the IIIa/IIa ratio may serve a better proxy for
361 quantifying soil organic carbon than the BIT index because it is less affected by
362 selective degradation of branched vs. isoprenoid GDGTs and high production of
363 crenarchaea in marine environments (Smith et al., 2012).

364

365 4 Conclusions

366 Based on a detailed study on GDGTs for three cores in the Bohai Sea and
367 compiling of GDGT data from globally distributed soils and marine sediments, we have
368 reached several important conclusions. Firstly, the ratio of brGDGTs IIIa/IIa is
369 generally lower than 0.59 in soils, but higher than 0.92 in marine sediments devoid of
370 significant terrestrial inputs, making it a sensitive proxy for assessing soil vs. marine
371 derived brGDGTs at regional and global scales. Secondly, in situ production of
372 brGDGTs in marine environments is a ubiquitous phenomenon, which is particularly
373 important for those marine sediments with low BIT index (<0.16) where brGDGTs are
374 exclusively of a marine origin. Thirdly, a systemic difference of the IIIa/IIa value
375 between soils and marine sediments reflects an influence of pH rather than temperature
376 on the biosynthesis of brGDGTs by source organisms. Given these facts, we strongly
377 recommend to calculate the IIIa/IIa ratio before estimating organic carbon source,
378 paleo-soil pH and MAT based on the BIT and MBT/CBT proxies.

379

380 Acknowledgements. The work was financially supported by the National Science
381 Foundation of China (41476062). We are grateful for X. Dang for GDGT analyses. G.



382 Jia, J. Hu, A. Leider, G. Mollenhauer, G. Trommer and R. Smith are thanked for kindly
383 supplying GDGT data.

384

385 References

386 Belicka, L.L., Harvey, H.R., 2009. The sequestration of terrestrial organic carbon in Arctic Ocean
387 sediments: A comparison of methods and implications for regional carbon budgets. *Geochimica Et*
388 *Cosmochimica Acta* 73, 6231–6248.

389 Blaga, C.I., Reichart, G.J., Vissers, E.W., Lotter, A.F., Anselmetti, F.S., Damste, J.S.S., 2011. Seasonal
390 changes in glycerol dialkyl glycerol tetraether concentrations and fluxes in a perialpine lake: Implications
391 for the use of the TEX86 and BIT proxies. *Geochimica Et Cosmochimica Acta* 75, 6416–6428.

392 Chen, W., Mohtadi, M., Schefuß, E., Mollenhauer, G., 2014. Organic-geochemical proxies of sea surface
393 temperature in surface sediments of the tropical eastern Indian Ocean. *Deep Sea Research Part I:*
394 *Oceanographic Research Papers* 88, 17–29.

395 Coffinet, S., Huguet, A., Williamson, D., Fosse, C., Derenne, S., 2014. Potential of GDGTs as a
396 temperature proxy along an altitudinal transect at Mount Rungwe (Tanzania). *Organic Geochemistry* 68,
397 82–89.

398 De Jonge, C., Hopmans, E.C., Stadnitskaia, A., Rijpstra, W.I.C., Hofland, R., Tegelaar, E., Sinninghe
399 Damsté, J.S., 2013. Identification of novel penta- and hexamethylated branched glycerol dialkyl glycerol
400 tetraethers in peat using HPLC–MS2, GC–MS and GC–SMB-MS. *Organic Geochemistry* 54, 78–82.

401 De Jonge, C., Hopmans, E.C., Zell, C.I., Kim, J.-H., Schouten, S., Sinninghe Damsté, J.S., 2014.
402 Occurrence and abundance of 6-methyl branched glycerol dialkyl glycerol tetraethers in soils:
403 Implications for palaeoclimate reconstruction. *Geochimica et Cosmochimica Acta* 141, 97–112.

404 De Jonge, C., Stadnitskaia, A., Cherkashov, G., Sinninghe Damsté, J.S., 2016. Branched glycerol dialkyl
405 glycerol tetraethers and crenarchaeol record post-glacial sea level rise and shift in source of terrigenous
406 brGDGTs in the Kara Sea (Arctic Ocean). *Organic Geochemistry* 92, 42–54.

407 De Jonge, C., Stadnitskaia, A., Hopmans, E.C., Cherkashov, G., Fedotov, A., Streletskaya, I.D., Vasiliev,
408 A.A., Sinninghe Damsté, J.S., 2015. Drastic changes in the distribution of branched tetraether lipids in
409 suspended matter and sediments from the Yenisei River and Kara Sea (Siberia): Implications for the use
410 of brGDGT-based proxies in coastal marine sediments. *Geochimica et Cosmochimica Acta* 165, 200–
411 225.



- 412 Ding, S., Xu, Y., Wang, Y., He, Y., Hou, J., Chen, L., He, J.S., 2015. Distribution of branched glycerol
413 dialkyl glycerol tetraethers in surface soils of the Qinghai–Tibetan Plateau: implications of brGDGTs-
414 based proxies in cold and dry regions. *Biogeosciences* 12, 3141–3151.
- 415 Dong, L., Li, Q., Li, L., Zhang, C.L., 2015. Glacial–interglacial contrast in MBT/CBT proxies in the
416 South China Sea: Implications for marine production of branched GDGTs and continental teleconnection.
417 *Organic Geochemistry* 79, 74–82.
- 418 Fietz, S., Huguet, C., Bendle, J., Escala, M., Gallacher, C., Herfort, L., Jamieson, R., Martínez-García,
419 A., McClymont, E.L., Peck, V.L., Prah, F.G., Rossi, S., Rueda, G., Sanson-Barrera, A., Rosell-Melé, A.,
420 2012. Co-variation of crenarchaeol and branched GDGTs in globally-distributed marine and freshwater
421 sedimentary archives. *Global and Planetary Change* 92–93, 275–285.
- 422 Fietz, S., Prah, F.G., Moraleda, N., Rosell-Melé, A., 2013. Eolian transport of glycerol dialkyl glycerol
423 tetraethers (GDGTs) off northwest Africa. *Organic Geochemistry* 64, 112–118.
- 424 French, D.W., Huguet, C., Turich, C., Wakeham, S.G., Carlson, L.T., Ingalls, A.E., 2015a. Spatial
425 distributions of core and intact glycerol dialkyl glycerol tetraethers (GDGTs) in the Columbia River
426 Basin and Willapa Bay, Washington: Insights into origin and implications for the BIT index. *Organic*
427 *Geochemistry* 88, 91–112.
- 428 French, D.W., Huguet, C., Wakeham, S., Turich, C., Carlson, L.T., Ingalls, A.E., 2015b. Spatial
429 distributions of core and intact glycerol dialkyl glycerol tetraethers (GDGTs) in the Columbia River basin,
430 Washington: Insights into origin and implications for the BIT index, EGU General Assembly Conference,
431 pp. 91–112.
- 432 Herfort, L., Schouten, S., Boon, J.P., Woltering, M., Baas, M., Weijers, J.W.H., Damsté, J.S.S., 2006.
433 Characterization of transport and deposition of terrestrial organic matter in the southern North Sea using
434 the BIT index. *Limnology & Oceanography* 51, 2196–2205.
- 435 Hopmans, E.C., Weijers, J.W.H., Schefuss, E., Herfort, L., Damsté, J.S.S., Schouten, S., 2004. A novel
436 proxy for terrestrial organic matter in sediments based on branched and isoprenoid tetraether lipids. *Earth*
437 *and Planetary Science Letters* 224, 107–116.
- 438 Hu, J., Meyers, P.A., Chen, G., Peng, P.A., Yang, Q., 2012. Archaeal and bacterial glycerol dialkyl
439 glycerol tetraethers in sediments from the Eastern Lau Spreading Center, South Pacific Ocean. *Organic*
440 *Geochemistry* 43, 162–167.
- 441 Hu, J., Zhou, H., Peng, P.a., Spiro, B., 2016. Seasonal variability in concentrations and fluxes of glycerol



442 dialkyl glycerol tetraethers in Huguangyan Maar Lake, SE China: Implications for the applicability of
443 the MBT–CBT paleotemperature proxy in lacustrine settings. *Chemical Geology* 420, 200–212.

444 Hu, L., Guo, Z., Feng, J., Yang, Z., Fang, M., 2009. Distributions and sources of bulk organic matter and
445 aliphatic hydrocarbons in surface sediments of the Bohai Sea, China. *Marine Chemistry* 113, 197–211.

446 Huguet, A., Fosse, C., Metzger, P., Fritsch, E., Derenne, S., 2010. Occurrence and distribution of
447 extractable glycerol dialkyl glycerol tetraethers in podzols. *Organic Geochemistry* 41, 291–301.

448 Huguet, C., de Lange, G.J., Gustafsson, Ö., Middelburg, J.J., Sinninghe Damsté, J.S., Schouten, S., 2008.
449 Selective preservation of soil organic matter in oxidized marine sediments (Madeira Abyssal Plain).
450 *Geochimica et Cosmochimica Acta* 72, 6061–6068.

451 Huguet, C., Kim, J.-H., de Lange, G.J., Sinninghe Damsté, J.S., Schouten, S., 2009. Effects of long term
452 oxic degradation on the , TEX₈₆ and BIT organic proxies. *Organic Geochemistry* 40, 1188–1194.

453 Jia, G., Zhang, J., Chen, J., Peng, P.A., Zhang, C.L., 2012. Archaeal tetraether lipids record subsurface
454 water temperature in the South China Sea. *Organic Geochemistry* 50, 68–77.

455 Kaiser, J., Schouten, S., Kilian, R., Arz, H.W., Lamy, F., Sinninghe Damsté, J.S., 2015. Isoprenoid and
456 branched GDGT-based proxies for surface sediments from marine, fjord and lake environments in Chile.
457 *Organic Geochemistry* 89–90, 117–127.

458 Kim, J.H., Meer, J.V.D., Schouten, S., Helmke, P., Willmott, V., Sangiorgi, F., Koç, N., Hopmans, E.C.,
459 Damsté, J.S.S., 2010. New indices and calibrations derived from the distribution of crenarchaeal
460 isoprenoid tetraether lipids: Implications for past sea surface temperature reconstructions. *Geochimica*
461 *Et Cosmochimica Acta* 74, 4639–4654.

462 Kim, J.H., Schouten, S., Buscail, R., Ludwig, W., Bonnin, J., Sinninghe Damsté, J.S., Bourrin, F., 2006.
463 Origin and distribution of terrestrial organic matter in the NW Mediterranean (Gulf of Lions): Exploring
464 the newly developed BIT index. *Geochemistry Geophysics Geosystems* 7, 220–222.

465 Leider, A., Hinrichs, K.U., Mollenhauer, G., Versteegh, G.J.M., 2010. Core-top calibration of the lipid-
466 based UK'37 and TEX₈₆ temperature proxies on the southern Italian shelf (SW Adriatic Sea, Gulf of
467 Taranto). *Earth & Planetary Science Letters* 300, 112–124.

468 Lincoln, S.A., Wai, B., Eppley, J.M., Church, M.J., Summons, R.E., Delong, E.F., 2014. Planktonic
469 Euryarchaeota are a significant source of archaeal tetraether lipids in the ocean. *Proceedings of the*
470 *National Academy of Sciences* 111, 9858–9863.

471 Lipp, J.S., Morono, Y., Inagaki, F., Hinrichs, K.U., 2008. Significant contribution of Archaea to extant



- 472 biomass in marine subsurface sediments. *Nature* 454, 991–994.
- 473 Liu, X.-L., Zhu, C., Wakeham, S.G., Hinrichs, K.-U., 2014. In situ production of branched glycerol
474 dialkyl glycerol tetraethers in anoxic marine water columns. *Marine Chemistry* 166, 1–8.
- 475 Loomis, S.E., Russell, J.M., Damsté, J.S.S., 2011. Distributions of branched GDGTs in soils and lake
476 sediments from western Uganda: Implications for a lacustrine paleothermometer. *Organic Geochemistry*
477 42, 739–751.
- 478 Meyers, P.A., 1997. Organic geochemical proxies of paleoceanographic, paleolimnologic, and
479 paleoclimatic processes. *Organic Geochemistry* 27, 213–250.
- 480 Mueller-Niggemann, C., Utami, S.R., Marxen, A., Mangelsdorf, K., Bauersachs, T., Schwark, L., 2016.
481 Distribution of tetraether lipids in agricultural soils—differentiation between paddy and upland
482 management. *Biogeosciences* 13, 1647–1666.
- 483 O'Brien, C.L., Foster, G.L., Martínez-Boti, M.A., Abell, R., Rae, J.W.B., Pancost, R.D., 2014. High sea
484 surface temperatures in tropical warm pools during the Pliocene. *Nature Geoscience* 7, 606–611.
- 485 Peterse, F., Kim, J.-H., Schouten, S., Kristensen, D.K., Koç, N., Sinninghe Damsté, J.S., 2009a.
486 Constraints on the application of the MBT/CBT palaeothermometer at high latitude environments
487 (Svalbard, Norway). *Organic Geochemistry* 40, 692–699.
- 488 Peterse, F., Schouten, S., van der Meer, J., van der Meer, M.T.J., Sinninghe Damsté, J.S., 2009b.
489 Distribution of branched tetraether lipids in geothermally heated soils: Implications for the MBT/CBT
490 temperature proxy. *Organic Geochemistry* 40, 201–205.
- 491 Peterse, F., van der Meer, J., Schouten, S., Weijers, J.W.H., Fierer, N., Jackson, R.B., Kim, J.-H.,
492 Sinninghe Damsté, J.S., 2012. Revised calibration of the MBT–CBT paleotemperature proxy based on
493 branched tetraether membrane lipids in surface soils. *Geochimica et Cosmochimica Acta* 96, 215–229.
- 494 Peterse, F., Vonk, J.E., Holmes, R.M., Giosan, L., Zimov, N., Eglinton, T.I., 2014. Branched glycerol
495 dialkyl glycerol tetraethers in Arctic lake sediments: Sources and implications for paleothermometry at
496 high latitudes. *Journal of Geophysical Research: Biogeosciences* 119, 1738–1754.
- 497 Ren, M.-E., Shi, Y.-L., 1986. Sediment discharge of the Yellow River (China) and its effect on the
498 sedimentation of the Bohai and the Yellow Sea. *Continental Shelf Research* 6, 785–810.
- 499 Schouten, S., Hopmans, E.C., Baas, M., Boumann, H., Standfest, S., Konneke, M., Stahl, D.A.,
500 Sinninghe Damsté, J.S., 2008. Intact membrane lipids of "Candidatus Nitrosopumilus maritimus," a
501 cultivated representative of the cosmopolitan mesophilic group I Crenarchaeota. *Applied and*



- 502 Environmental Microbiology 74, 2433–2440.
- 503 Schouten, S., Hopmans, E.C., Schefuß, E., Sinninghe Damsté, J.S., 2002. Distributional variations in
504 marine crenarchaeotal membrane lipids: a new tool for reconstructing ancient sea water temperatures?
505 Earth and Planetary Science Letters 204, 265–274.
- 506 Schouten, S., Hopmans, E.C., Sinninghe Damsté, J.S., 2013. The organic geochemistry of glycerol
507 dialkyl glycerol tetraether lipids: A review. Organic Geochemistry 54, 19–61.
- 508 Sinninghe Damsté, J.S., 2016. Spatial heterogeneity of sources of branched tetraethers in shelf systems:
509 The geochemistry of tetraethers in the Berau River delta (Kalimantan, Indonesia). Geochimica et
510 Cosmochimica Acta 186, 13–31.
- 511 Sinninghe Damsté, J.S., Hopmans, E.C., Pancost, R.D., Schouten, S., Geenevasen, J.A.J., 2000. Newly
512 discovered non-isoprenoid glycerol dialkyl glycerol tetraether lipids in sediments. Chemical
513 Communications, 1683–1684.
- 514 Sinninghe Damsté, J.S., Ossebaar, J., Abbas, B., Schouten, S., Verschuren, D., 2009. Fluxes and
515 distribution of tetraether lipids in an equatorial African lake: Constraints on the application of the TEX86
516 palaeothermometer and BIT index in lacustrine settings. Geochimica et Cosmochimica Acta 73, 4232–
517 4249.
- 518 Sinninghe Damsté, J.S., Ossebaar, J., Schouten, S., Verschuren, D., 2008. Altitudinal shifts in the
519 branched tetraether lipid distribution in soil from Mt. Kilimanjaro (Tanzania): Implications for the
520 MBT/CBT continental palaeothermometer. Organic Geochemistry 39, 1072–1076.
- 521 Sinninghe Damsté, J.S., Rijpstra, W.I.C., Hopmans, E.C., Weijers, J.W.H., Foesel, B.U., Overmann, J.,
522 Dedysh, S.N., 2011. 13,16-Dimethyl Octacosanedioic Acid (iso-Diabolic Acid), a Common Membrane-
523 Spanning Lipid of Acidobacteria Subdivisions 1 and 3. Applied and Environmental Microbiology 77,
524 4147–4154.
- 525 Sinninghe Damsté, J.S., Schouten, S., Hopmans, E.C., van Duin, A.C.T., Geenevasen, J.A.J., 2002.
526 Crenarchaeol: the characteristic core glycerol dibiphytanyl glycerol tetraether membrane lipid of
527 cosmopolitan pelagic crenarchaeota. Journal of Lipid Research 43, 1641–1651.
- 528 Smith, R.W., Bianchi, T.S., Li, X., 2012. A re-evaluation of the use of branched GDGTs as terrestrial
529 biomarkers: Implications for the BIT Index. Geochimica Et Cosmochimica Acta 80, 14–29.
- 530 Sofianos, S.S., Johns, W.E., Murray, S.P., 2002. Heat and freshwater budgets in the Red Sea from direct
531 observations at Bab el Mandeb. Deep Sea Research Part II: Topical Studies in Oceanography 49, 1323–



- 532 1340.
- 533 Sparkes, R.B., Doğrul Selver, A., Bischoff, J., Talbot, H.M., Gustafsson, Ö., Semiletov, I.P., Dudarev,
534 O.V., van Dongen, B.E., 2015. GDGT distributions on the East Siberian Arctic Shelf: implications for
535 organic carbon export, burial and degradation. *Biogeosciences* 12, 3753–3768.
- 536 Tierney, J.E., Russell, J.M., 2009. Distributions of branched GDGTs in a tropical lake system:
537 Implications for lacustrine application of the MBT/CBT paleoproxy. *Organic Geochemistry* 40, 1032–
538 1036.
- 539 Tierney, J.E., Schouten, S., Pitcher, A., Hopmans, E.C., Sinninghe Damsté, J.S., 2012. Core and intact
540 polar glycerol dialkyl glycerol tetraethers (GDGTs) in Sand Pond, Warwick, Rhode Island (USA):
541 Insights into the origin of lacustrine GDGTs. *Geochimica et Cosmochimica Acta* 77, 561–581.
- 542 Trommer, G., Siccha, M., Meer, M.T.J.V.D., Schouten, S., Damsté, J.S.S., Schulz, H., Hemleben, C.,
543 Kucera, M., 2009. Distribution of Crenarchaeota tetraether membrane lipids in surface sediments from
544 the Red Sea. *Organic Geochemistry* 40, 724–731.
- 545 Walsh, E.M., Ingalls, A.E., Keil, R.G., 2008. Sources and transport of terrestrial organic matter in
546 Vancouver Island fjords and the Vancouver-Washington Margin: A multiproxy approach using $\delta^{13}\text{C}_{\text{org}}$,
547 lignin phenols, and the ether lipid BIT index. *Limnology and Oceanography* 53, 1054–1063.
- 548 Weijers, J.W.H., Schefuß, E., Kim, J.-H., Sinninghe Damsté, J.S., Schouten, S., 2014. Constraints on the
549 sources of branched tetraether membrane lipids in distal marine sediments. *Organic Geochemistry* 72,
550 14–22.
- 551 Weijers, J.W.H., Schefuß, E., Schouten, S., Damsté, J.S.S., 2007a. Coupled Thermal and Hydrological
552 Evolution of Tropical Africa over the Last Deglaciation. *Science* 315, 1701–1704.
- 553 Weijers, J.W.H., Schouten, S., Donker, J.C.V.D., Hopmans, E.C., Damsté, J.S.S., 2007b. Environmental
554 controls on bacterial tetraether membrane lipid distribution in soils. *Geochimica Et Cosmochimica Acta*
555 71, 703–713.
- 556 Weijers, J.W.H., Schouten, S., Spaargaren, O.C., Sinninghe Damsté, J.S., 2006. Occurrence and
557 distribution of tetraether membrane lipids in soils: Implications for the use of the TEX86 proxy and the
558 BIT index. *Organic Geochemistry* 37, 1680–1693.
- 559 White, D.C., Davis, W.M., Nickels, J.S., King, J.D., Bobbie, R.J., 1979. Determination of the
560 sedimentary microbial biomass by extractible lipid phosphate. *Oecologia* 40, 51–62.
- 561 Wu, W., Ruan, J., Ding, S., Zhao, L., Xu, Y., Yang, H., Ding, W., Pei, Y., 2014. Source and distribution



562 of glycerol dialkyl glycerol tetraethers along lower Yellow River-estuary-coast transect. *Marine*
563 *Chemistry* 158, 17–26.

564 Wu, W., Zhao, L., Pei, Y., Ding, W., Yang, H., Xu, Y., 2013. Variability of tetraether lipids in Yellow
565 River-dominated continental margin during the past eight decades: Implications for organic matter
566 sources and river channel shifts. *Organic Geochemistry* 60, 33–39.

567 Xiao, W., Xu, Y., Ding, S., Wang, Y., Zhang, X., Yang, H., Wang, G., Hou, J., 2015. Global calibration
568 of a novel, branched GDGT-based soil pH proxy. *Organic Geochemistry* 89–90, 56–60.

569 Yang, G., Zhang, C.L., Xie, S., Chen, Z., Gao, M., Ge, Z., Yang, Z., 2013. Microbial glycerol dialkyl
570 glycerol tetraethers lipids from water and soil at the Three Gorges Dam on the Yangtze River. *Organic*
571 *Geochemistry* 56, 40–50.

572 Yang, H., Pancost, R.D., Dang, X., Zhou, X., Evershed, R.P., Xiao, G., Tang, C., Gao, L., Guo, Z., Xie,
573 S., 2014a. Correlations between microbial tetraether lipids and environmental variables in Chinese soils:
574 Optimizing the paleo-reconstructions in semi-arid and arid regions. *Geochimica et Cosmochimica Acta*
575 126, 49–69.

576 Yang, H., Pancost, R.D., Tang, C., Ding, W., Dang, X., Xie, S., 2014b. Distributions of isoprenoid and
577 branched glycerol dialkanol diethers in Chinese surface soils and a loess–paleosol sequence: Implications
578 for the degradation of tetraether lipids. *Organic Geochemistry* 66, 70–79.

579 Zell, C., Kim, J.-H., Dorhout, D., Baas, M., Sinninghe Damsté, J.S., 2015. Sources and distributions of
580 branched tetraether lipids and crenarchaeol along the Portuguese continental margin: Implications for the
581 BIT index. *Continental Shelf Research* 96, 34–44.

582 Zell, C., Kim, J.-H., Hollander, D., Lorenzoni, L., Baker, P., Silva, C.G., Nittrouer, C., Sinninghe Damsté,
583 J.S., 2014. Sources and distributions of branched and isoprenoid tetraether lipids on the Amazon shelf
584 and fan: Implications for the use of GDGT-based proxies in marine sediments. *Geochimica et*
585 *Cosmochimica Acta* 139, 293–312.

586 Zhang, Y.G., Zhang, C.L., Liu, X.-L., Li, L., Hinrichs, K.-U., Noakes, J.E., 2011. Methane Index: A
587 tetraether archaeal lipid biomarker indicator for detecting the instability of marine gas hydrates. *Earth*
588 *and Planetary Science Letters* 307, 525–534.

589 Zhu, C., Wakeham, S.G., Elling, F.J., Basse, A., Mollenhauer, G., Versteegh, G.J.M., Ouml, nneke, M.,
590 Hinrichs, K.U., 2016. Stratification of archaeal membrane lipids in the ocean and implications for
591 adaptation and chemotaxonomy of planktonic archaea. *Environmental Microbiology*, DOI:



592 10.1111/1462-2920.13289.

593 Zhu, C., Weijers, J.W.H., Wagner, T., Pan, J.M., Chen, J.F., Pancost, R.D., 2011. Sources and distributions

594 of tetraether lipids in surface sediments across a large river-dominated continental margin. *Organic*

595 *Geochemistry* 42, 376–386.

596

597

598

599

600

601

602

603

604

605

606

607

608

609

610

611

612

613

614

615

616

617

618

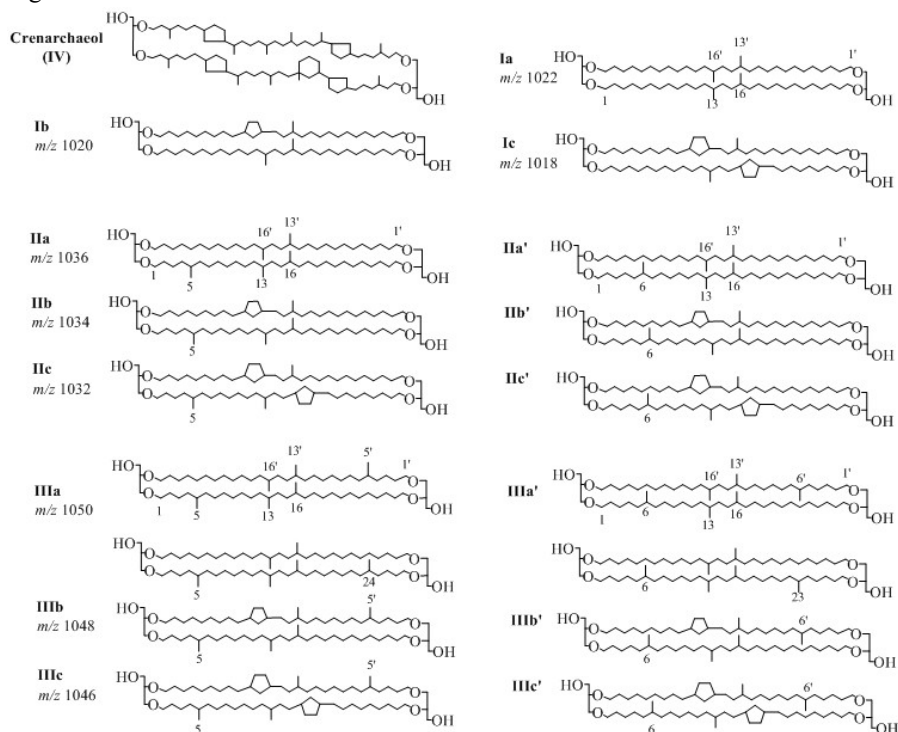
619

620

621



622 Fig.1. Chemical structures of branched GDGTs and crenarchaeol.



623

624

625

626

627

628

629

630

631

632

633

634

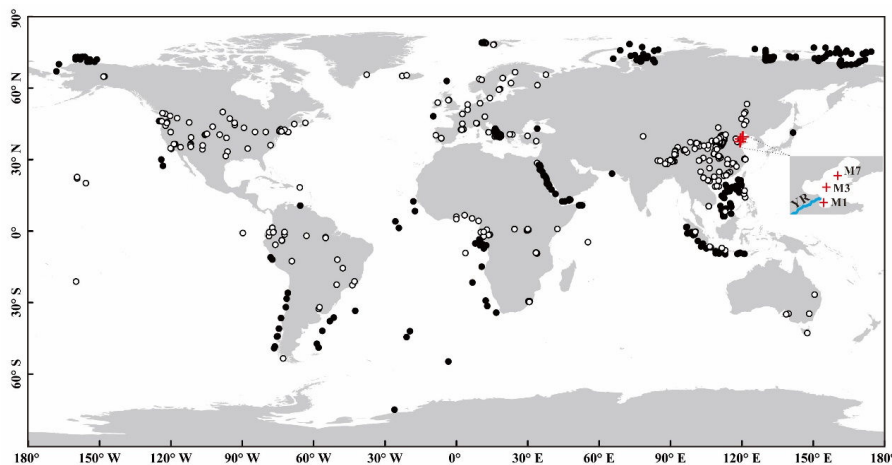
635

636

637



638 Fig.2. Location of the samples used in this study. White circles and black circles
639 indicate the soils and marine sediments, respectively. Red crosses denote three sediment
640 cores (M1, M3 and M7) in the Bohai Sea. YR is the Yellow River.



641

642

643

644

645

646

647

648

649

650

651

652

653

654

655

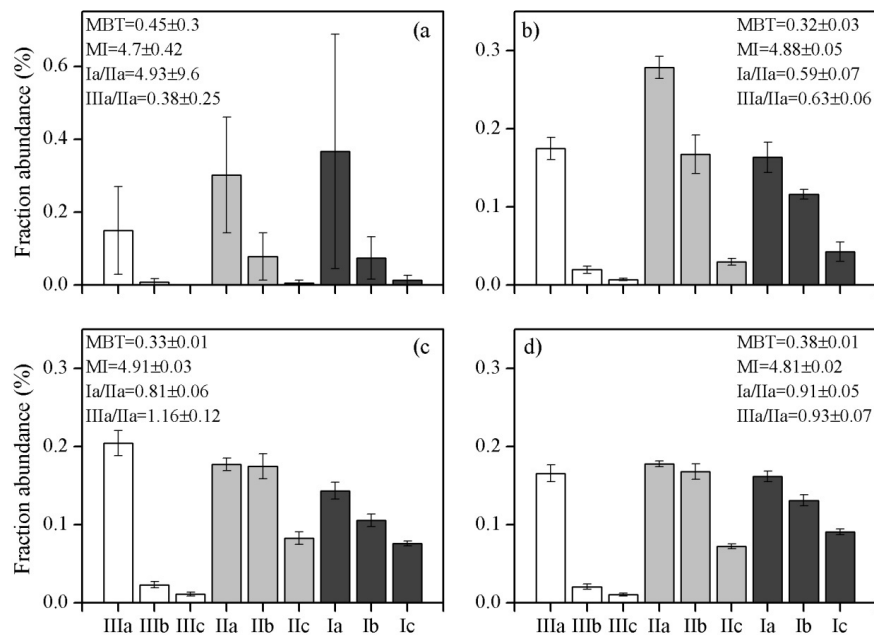
656

657

658



659 Fig.3. Averaged percentages of individual brGDGTs in soils (a), core M1 (b), M3 (c)
660 and M7 (d). The soil data are from Yang et al. (2014a).



661

662

663

664

665

666

667

668

669

670

671

672

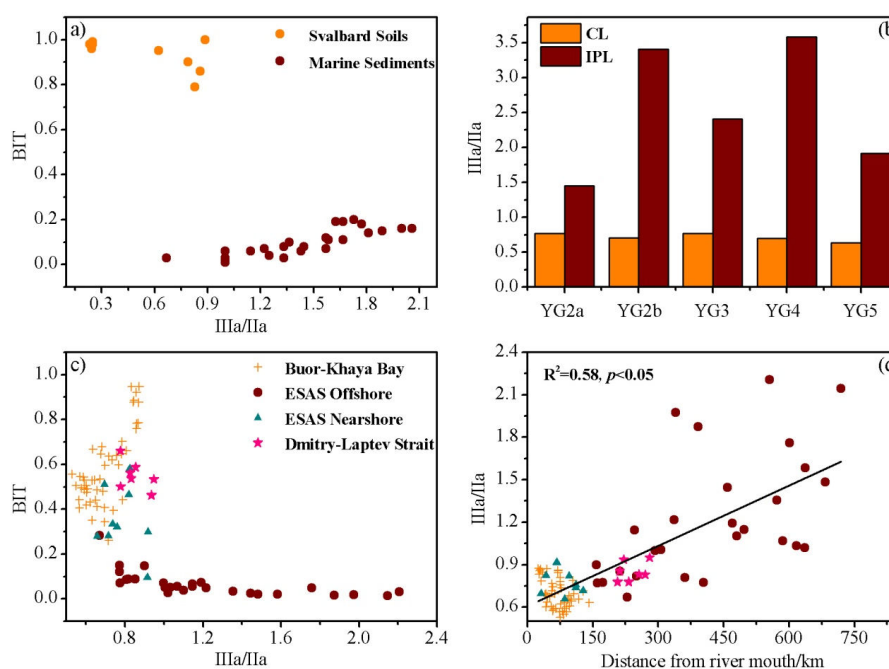
673

674

675



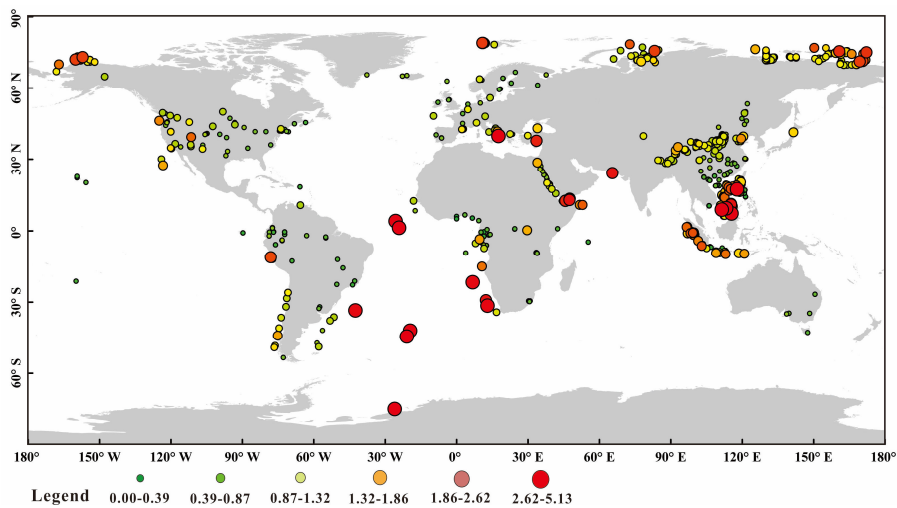
676 Fig. 4. a) The relationship between brGDGT IIIa/IIa ratio and the BIT index of samples
677 from Peterse et al. (2009a); b) histograms of brGDGT IIIa/IIa ratio of the core lipids
678 (CLs) and intact polar lipids (IPLs) in samples from De Jonge et al. (2015); c) the
679 relationship between brGDGT IIIa/IIa ratio and the BIT index in samples from Sparkes
680 et al. (2015); d) the relationship between brGDGT IIIa/IIa ratio and distance from river
681 mouth in samples from Sparkes et al.(2015).



682
683
684
685
686
687
688
689
690
691
692



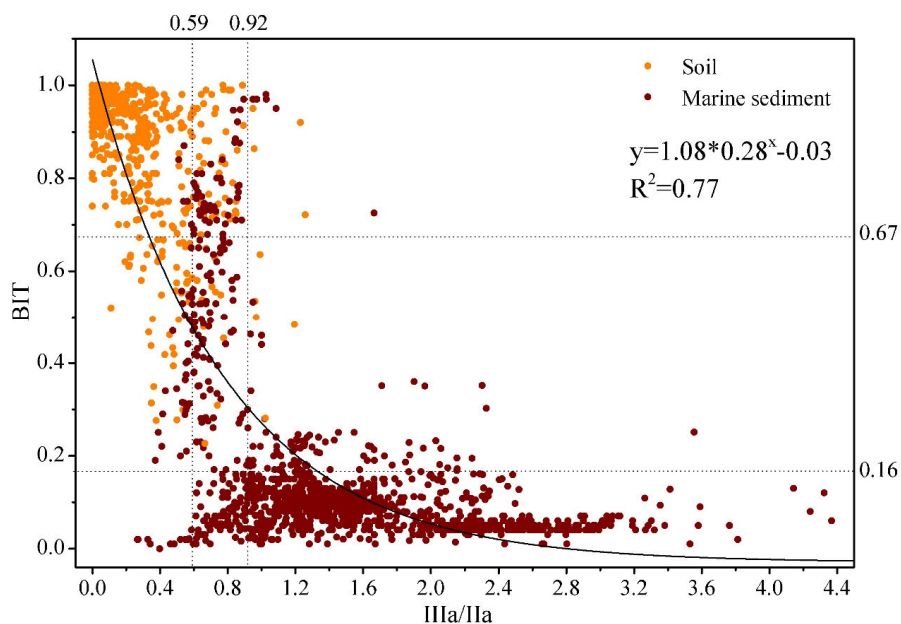
693 Fig. 5. Global distribution pattern of brGDGT IIIa/IIa ratio in soils and marine
694 sediments.



695
696
697
698
699
700
701
702
703
704
705
706
707
708
709
710
711
712
713



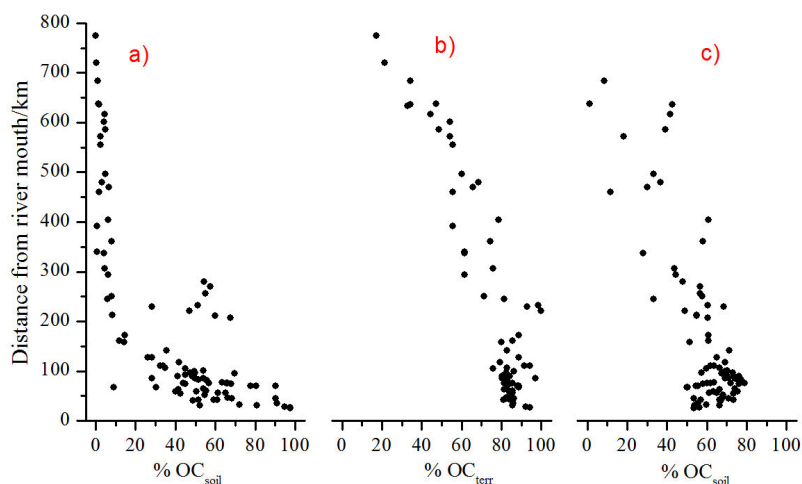
714 Fig. 6. Relationship between the IIIa/IIa ratio and the BIT index of globally distributed
715 samples: soils (orange circle) and marine sediments (red circle). Dashed lines represent
716 lower or upper threshold values for 90% of soils/sediments.



717
718
719
720
721
722
723
724
725
726
727
728
729
730
731



732 Fig. 7. Percentage of soil organic carbon (%OC_{soil}) or terrestrial organic carbon
733 (%OC_{terr}) based on a binary mixing model of BIT (a), $\delta^{13}\text{C}_{\text{org}}$ (b) and IIIa/IIa (c) for the
734 East Siberian Arctic Shelf (Sparkes et al., 2015).



735
736
737
738
739
740
741
742
743
744
745
746
747
748
749
750
751
752



753 Table 1: Parameters including brGDGTs IIIa/IIa, Ia/IIa, the BIT index, MBT, MI, DC,
 754 percentages of tetra-, penta- and hexa-methylated brGDGTs, and the weighted average
 755 number of cyclopentane moieties (#rings for tetramethylated brGDGTs) based on the
 756 GDGTs from three cores (M1, M3 and M7) in the Bohai Sea. Different letters (a, b, c,
 757 d) represent significant difference at the level of $p < 0.05$.

Indexes	Soil	M1	M3	M7
IIIa/IIa	0.39±0.25 (a)	0.63±0.06 (b)	1.16±0.12 (c)	0.93±0.07 (d)
Ia/IIa	4.93±9.60 (a)	0.59±0.07 (b)	0.81±0.06 (b)	0.91±0.05 (b)
BIT	0.75±0.22 (a)	0.50±0.19 (b)	0.14±0.06 (c)	0.11±0.03 (c)
MBT	0.45±0.30 (a)	0.32±0.03 (b)	0.33±0.01 (b)	0.38±0.01 (ab)
MI	4.70±0.42 (a)	4.88±0.05 (b)	4.91±0.03 (b)	4.81±0.02 (ab)
DC	0.31±0.21 (a)	0.62±0.03 (b)	0.79±0.03 (c)	0.82±0.02 (c)
%tetra	0.45±0.30 (a)	0.32±0.03 (b)	0.33±0.01 (c)	0.38±0.01 (c)
%hexa	0.16±0.12 (a)	0.20±0.02 (b)	0.24±0.02 (b)	0.20±0.01 (b)
%penta	0.39±0.20 (a)	0.48±0.02 (b)	0.44±0.02 (b)	0.42±0.01 (b)
#Rings _{tetra}	0.20±0.15 (a)	0.39±0.03 (b)	0.47±0.02 (c)	0.47±0.02 (c)

758

759